remote sensing

MDPI

Article

Mapping Decadal Land Cover Changes in the Woodlands of North Eastern Namibia from 1975 to 2014 Using the Landsat Satellite Archived Data

Vladimir R. Wingate [1,*], Stuart R. Phinn [2,†], Nikolaus Kuhn [1,†], Lena Bloemertz [1,†] and Kiran L. Dhanjal-Adams [3,†]

1 Physical Geography and Environmental Change, University of Basel, Klingelbergstrasse 27, Basel 4056, Switzerland; Nikolaus.kuhn@unibas.ch (N.K.); Lena.bloemertz@unibas.ch (L.B.)
2 Remote Sensing Research Centre, School of Geography, Planning and Environmental Management, The University of Queensland, St. Lucia, QLD 4072, Australia; s.phinn@uq.edu
3 Centre for Ecology and Hydrology, Maclean Building, Benson Lane, Crowmarsh Gifford, Wallingford, OX10 8BB Oxfordshire, UK; kiran.dhanjal.adams@gmail.com or kiradha@ceh.ac.uk
* Correspondence: Vladimir.wingate@unibas.ch; Tel.: +41-78-613-6259
† These authors contributed equally to this work.

Academic Editors: Parth Sarathi Roy, Clement Atzberger and Prasad S. Thenkabail
Received: 11 June 2016; Accepted: 15 August 2016; Published: 20 August 2016

Abstract: Woodlands and savannahs provide essential ecosystem functions and services to communities. On the African continent, they are widely utilized and converted to subsistence and intensive agriculture or urbanized. This study investigates changes in land cover over four administrative regions of North Eastern Namibia within the Kalahari woodland savannah biome, covering a total of 107,994 km^2. Land cover is mapped using multi-sensor Landsat imagery at decadal intervals from 1975 to 2014, with a post-classification change detection method. The dominant change observed was a reduction in the area of woodland savannah due to the expansion of agriculture, primarily in the form of small-scale cereal and pastoral production. More specifically, woodland savannah area decreased from 90% of the study area in 1975 to 83% in 2004, and then increased to 86% in 2014, while agricultural land increased from 6% to 12% between 1975 and 2014. We assess land cover changes in relation to towns, villages, rivers and roads and find most changes occurred in proximity to these. In addition, we find that most land cover changes occur within land designated as communally held, followed by state protected land. With widespread changes occurring across the African continent, this study provides important data for understanding drivers of change in the region and their impacts on the distribution of woodland savannahs.

Keywords: deforestation; land degradation; woodland; savannah; Landsat; land cover change; land-use change; Africa; Corona

1. Introduction

Human activities are altering the surface of the biosphere in profound ways. Whether by clearing forests, intensifying cropland production or expanding urban areas, anthropogenic activities have altered an increasingly large proportion of the Earth's land surface [1]. The effects of land surface changes range from alterations to the composition of the atmosphere and climate, to the loss of biodiversity and the disruption of biogeochemical cycles [2–4]. Due to the significance of such changes on the biosphere, monitoring changes in land cover is a high priority area for research [5]. In effect, maps and datasets which quantify biophysical variables, including land-use and land cover (LULC), are essential for understanding and modelling complex interactions and impacts between the natural and human environments, from regional to global scales. These include processes such as deforestation,

land degradation and landscape carbon dynamics in the context of global change [5–7]. Furthermore, multi-temporal analyses of LULC provide important insights into long term trends which serve to identify drivers and determinants of change [8,9]. Indeed, in regions where there is a lack of sufficiently detailed cartographic information, environmental change detection and monitoring using satellite data can be pivotal in providing a basis for planning, management and conservation initiatives [10]. In particular, satellite remote sensing using the Landsat system has been used extensively to quantify the extent of LULC in numerous environments around the world [11,12].

Across the African continent, the overall tendency has been toward the clearing of land, including savannah, for crop farming and grazing [13–16]. In the communally held regions of North Eastern Namibia, savannahs have declined due to small-scale cropland expansion, increased grazing, fire frequency and land-use pressure [17,18]. However, theses landscapes provide numerous important ecosystem goods and services upon which people depend [19–22]. We use the definition by [23] of the study area as falling within the Northern Kalahari woodland savannah and refer to the biome as woodland. Broadly, savannah biomes are characterized by a mixture of herbaceous and woodland plant functional groups, commonly consisting of a woody tree and shrub layer with a grassy or herbaceous understory, and with a forest canopy cover between 10% and 30%. Often arid to semi-arid, they undergo marked spatio-temporal shifts in climate and land-use, resulting in pronounced annual and inter-annual divergence of vegetation characteristics [24,25]. As a consequence, these ecosystems show some of the lowest satellite based land cover mapping accuracies in comparison to homogenous vegetation types [26,27]. Nevertheless, recent studies [18,28–32] have successfully used remote sensing data to assess changes in woodland and arable land cover in Northern Namibia. However, they have concentrated on mapping vegetation change within spatially restricted areas i.e., either a portion or single Namibian administrative region, and using short time scales, such as two time intervals. Indeed, land cover changes having occurred over the past 40 years have, to our knowledge, not yet been quantified at the landscape scale, and change trajectories among land cover classes explained and evaluated.

To address this gap and to gain an in-depth understanding of the magnitude and trajectory of land cover changes at a regional scale (10^4 km^2), we use Landsat archive satellite imagery, freely available from the United States Geological Survey (USGS). We explore land cover changes in North East (NE) Namibia over the past four decades (1975–2014) at decadal time scale intervals, using a post-classification change detection method. The aim is to map and discuss the changes in the main land cover types with an emphasis on woodland change. We identify increases in area under arable land and losses of woodland by measuring and assessing: (i) the area of change; (ii) the spatial distribution of change; (iii) the trajectories of change between land cover types; (iv) the potential drivers of change; and, finally, (v) the accuracy of the maps. Information resulting from this research can serve as a practical foundation for interpreting the underlying drivers of environmental change, developing strategies for the sustainable development of the region and informing policy and conservation initiatives. For example, these data provide details on the temporal and spatial patterns of land cover change processes, which can be used to assess the consequences of past, present, and future land-use policies, as well as providing a basis for quantifying landscape carbon dynamics.

2. Methods

The following section details the: (i) study area; (ii) data acquisition and processing; (iii) change detection work flow; (iv) land cover change analysis; (v) proximal variables of change analysis; and (vi) accuracy assessment.

2.1. Study Area

The study region is located within the Kalahari woodland savannah of NE Namibia [23,33] at the southern edge of the African "miombo" ecoregion, and upon the Kalahari sand sheet [34,35]. It extends over 107,994 km^2 to include the administrative regions of Ohangwena, Oshikoto, Kavango and Zambesi

(Caprivi) (Figure 1). The rationale for defining the boundaries of the study region is the overlap between the relatively homogenous eco-floristic and bioclimatic extent of the Kalahari woodland savannah and the common pattern of communal land use within these administrative regions. The communal farming sector is labour-intensive and subsistence-based, with limited mechanical and chemical inputs and user rather than ownership rights defining tenure. They are also characterised by a higher population density relative to other areas of Namibia [21,36]. The land is owned by the state but administered in trust by the communities and crop land is normally allocated to individual farmsteads while grazing land is shared between community members and is typically not fenced [21]. Agriculture throughout the region is characterized by agro-silvo-pastoralism centred on small-scale pearl millet (*Pennisetum glaucum*) cultivation, but also includes extensive cattle ranching and conventional irrigated agriculture [17]. Rain-fed crop farming is concentrated on certain soil types found near ephemeral rivers and clay pans which are more fertile than the surrounding deep sandy soils, while extensive grazing takes place in the remaining hinterland areas [32,37]. Logging in the region has taken place since the early 1900s, but the net cubic meter harvest has declined dramatically. Historically, large areas of woodland were cleared for crop farming, particularly in northern areas where soils and rainfall are better suited [38]. This trend continues and in recent decades new areas of woodland have been cleared for crops and settlements, with much of the deforestation taking place in two core areas, namely along the Okavango River and in western Ohangwena Region [29]. A rainfall gradient exists within the study area with a mean annual rainfall of 600 mm in the east to 400 mm in the west, and equally from north to south. Rainfall is concentrated from December to March but cumulative amounts vary greatly from year to year. Evapotranspiration rates are elevated and flooding affects a large proportion of the landscape, including primarily the Cuvelai basin and the region of Zambesi, resulting in large, ephemeral water and wetland bodies and pronounced variation in maximum plant growth and production [39]. Woody species are generally semi-deciduous or deciduous, with the western areas being dominated by *Colophospermum mopane* shrub-land and eastern areas by *Burkea africana*, *Baikiaea plurijuga*, *Pterocarpus angolensis* and *Guibourtia coleosperma*, woodland savannah [32,33]. Fire has a large impact on the landscape, for example, it was found that between 27% and 51% of the regions of Kavango and Zambesi burned annually between 1989 and 2001, resulting in reduced regeneration and tree mortality [40].

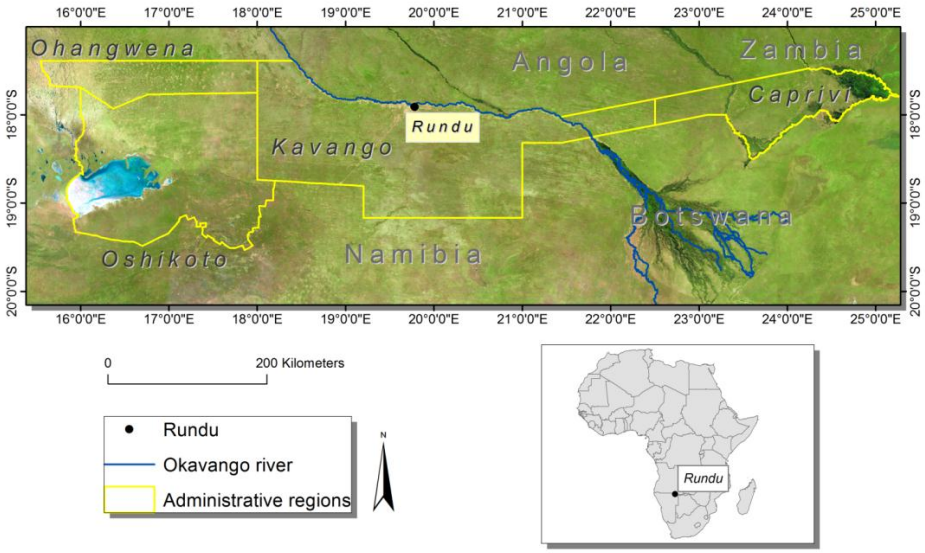

Figure 1. Study site, including four administrative regions of Ohangwena, Oshikoto, Kavango and Caprivi (**yellow**) and the Okavango River (**blue**) in North East (NE) Namibia. The map background is a Landsat 8 Top of the Atmosphere (TOA) reflectance, median composite, 60 m resolution image mosaic comprised of all scenes available for 2015 using the infrared bands 5, 4 and 3.

2.2. Landsat Scene Acquisition and Processing

Landsat Multispectral Scanner System (MSS), Thematic Mapper (TM), Enhanced Thematic Mapper Plus (ETM+) and Landsat 8 Operational Land Imager (OLI) scenes were obtained from the USGS, which are level 1 terrain corrected products (L1T) and offer acceptable levels of spatial accuracy, therefore no geo-rectification was required and image-to-image registration was omitted [41]. Digital numbers were converted to calibrated top of the atmosphere radiances and then corrected for atmospheric effects using the Apparent Reflectance Model, which makes no corrections for atmospheric scattering or absorption (an atmospheric transmittance value of 1, a path radiance due to haze of 0 and a spectral diffuse sky irradiance of 0 were used), resulting in an image of proportional reflectance [42]. Cloud free MSS images from the 1975 period were used whenever a suitable image was identified, i.e., one scene was acquired for 1973 and two for 1979, due to their limited availability and quality.

Pre-processed Landsat imagery available through Google's Earth Engine was used to assess LULC change across the study area. Here, Top of the Atmosphere (TOA) composite images were processed using all the available Landsat images for each year (i.e., 1984–1985), for the periods of 1984, 1994, 2004 and 2014. A cloud score was then applied to each pixel using the Simple Landsat Cloud Score algorithm, which selects the lowest possible range of cloud scores at each point and then computes per-band percentile values (i.e., the percentile value to use when compositing each band) from the accepted pixels. This algorithm also uses the Landsat Path Row Limit method to select only the least-cloudy scenes. The median pixel value of the composite image stack was then selected to carry out the analysis, in order to remove the influence of clouds, reduce image noise, cloud and fire scars. This results in multi-band images where each pixel represents the median of all unmasked pixels for each band. Finally, the new images were stacked with a normalized difference vegetation index (NDVI) band generated using the same method [43].

2.3. Classification and Change Detection Work Flow

To obtain a matrix of change between land cover classes, we used the post-classification method at decadal intervals [44]. A decadal time scale was chosen for several reasons: (i) a lack of cloud free, good quality images for this region, especially at the start of the Landsat archive; and (ii) the necessity to generate a regular time-series for the whole region. Here, we found decadal intervals provided seamless mosaics over the study region because limited imagery for the late 1970s and early 1980s period precluded generating a denser time series. We use the post-classification method to quantify land cover conversions, in which independently generated classifications at two time intervals are compared. The main advantage is to limit issues associated with radiometric calibration (i.e. solar illumination, atmospheric absorption and scattering and sensor properties) in between intervals [45]. However, the accuracy of the initial classification will dictate the accuracy of the post-classification comparison. In effect, the end accuracy approximates the compounding of the accuracies of every single classification. The complication thereby rests with producing regular, comparable and accurate results for every comparison [11].

Initially, a preliminary change detection study was carried out over a pilot area (11,240 km^2) on the border between the Ohangwena and Oshikoto administrative regions, known to be experiencing land cover changes. This was done to facilitate: (i) land cover class definition; (ii) the selection of suitable change detection methods; (iii) the identification of applicable image processing; and (iv) an initial accuracy assessment, as field data validation points had been collected in this area [28]. The area was encompassed by a single Landsat footprint and four scenes at decadal intervals between 1984 and 2014. Cloud free images from the early dry season and end of the wet season are considered the best for identifying woody vegetation in NE Namibia (April–May), as they maximize the contrast between the dry herbaceous layer and green canopy layer [33]. For this pilot study, Landsat TM, ETM+ and OLI scenes as close to the month of June were used due to scene availability. Five initial land cover classes were identified and scenes were classified using a supervised Maximum

Likelihood algorithm, with 10 training areas identified per class using Google Earth, aerial images loaned by the University of Namibia and 61 GPS points derived from field visits (Figure 2A).

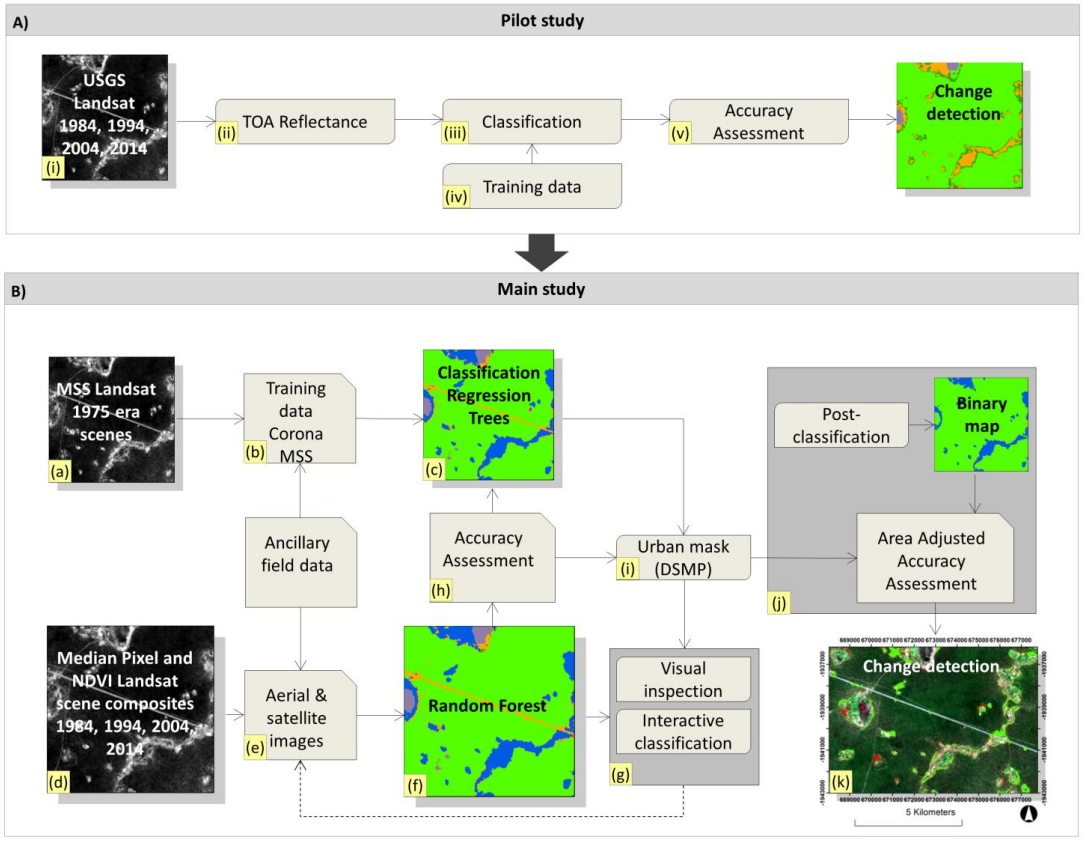

Figure 2. Workflow diagram illustrating the steps and methods employed. Pilot study (**A**): (i) Dry season (June) Landsat images at decadal intervals (1984–2014); (ii) processed to Top of the Atmosphere Reflectance (TOA); (iii) training data from Google Earth, aerial imagery and field Global Position system (GPS) points; (iv) classified with a supervised maximum likelihood classifier; and (v) accuracy assessment: validating 50 random sample points per class using available satellite and aerial imagery. Main study (**B**): (a) Cloud free (Multispectral Scanner system (MSS) scenes from the 1975 era; (b) training data derived from MSS scenes and Corona imagery; (c) Classification and Regression Tree (CART) classifiers; (d) for periods 1984–2014, all available Landsat scenes for one year (i.e., 1984–1985) were cloud masked and composited into a new image using the median pixel value and an Normalized Difference Vegetation Index (NDVI) band derived using the same method; (e) training data were interactively identified from Landsat scenes, Google Earth and aerial imagery, as well as ancillary knowledge from field visits; (f) Random Forest (RF) classifiers; (g) visual inspection and interactive classification (i.e., selection of training areas, and subsequent image classification); (h) accuracy assessment; (i) urban mask; (j) area adjusted accuracy assessment on post-classification binary maps; and (k) change area detection.

Machine-learning techniques, including Classification and Regression Trees (CART) and Random Forest (RF) are increasingly used to classify remotely sensed data and RF has been shown to improve classification accuracy [46]. Due to spectral differences between MSS scenes, it was not possible to composite all available images for the 1975 period, therefore, selected MSS scenes representing the period between 1973 and 1979 were classified individually using a CART classifier and reference Corona satellite photographs [47]. For the remaining periods (1984–2014) the median composite/NDVI image stacks were classified into the major land cover classes, using supervised RF classifiers and up to 8 training areas per class [46,48] (Table S1 in the Supplementary Material). Seven land cover classes

were selected in an attempt to capture the main landscape variability based on visual interpretation of high resolution satellite imagery and field visits (Table 1).

Table 1. Land cover classes used in the final analysis.

Class	Description
Water	Rivers, lakes and standing water bodies
Clay pan	Dry lake bed; layer of clay alternating with water during the wet season
Agriculture	Arable cropland, orchards and pasture, villages and farmsteads
Bare ground	Exposed sands, beaches, riparian sand bars, dunes and roads
Woodland	Predominant land cover class; includes all savannah woodland transitions
Wetland	Seasonally flooded areas found adjacent to rivers and lakes
Urban	Densely populated areas, paved roads, concrete, warehouses, and tarmac (masked)

Classes include" (i) "Water", which represents rivers, lakes and standing water bodies; (ii) "Clay pan", which denotes commonly found dry lake beds associated with drainage channels (often containing water from during the wet season), composed of eutric Arenosols with a high clay content (between 5% and 8%) [48]; (iii) "Agriculture", which designates a mosaic of arable cropland, orchards and pasture; includes, villages and farmsteads; (iv) "Bare ground", attempts to capture areas of sand, beaches, riparian sand bars, dunes and unpaved roads, all of which are spectrally distinct; (v) "Woodland", describes a heterogeneous savannah land cover type, i.e., savannahs, woodlands and transitions at different stages of disturbance and recovery; (vi) "Wetland", signifies permanently or seasonally flooded areas, often found adjacent to rivers and lakes and showing high NDVI values; and (vii) "Urban", attempts to estimate the extent of densely populated areas, which are often characterised by paved roads, warehouses and houses made of concrete brick as well as tarmac, by creating a mask based on Version 4 of the Defence Meteorological Program (DMSP) Operational Line scan System (OLS) Night time Lights Time Series [49]. Spectral separation between classes was not assessed in this study. Training sites were selected interactively, based on Landsat scenes, Google Earth imagery, aerial images and knowledge of land covers gained from previous field visits (Figure 2B).

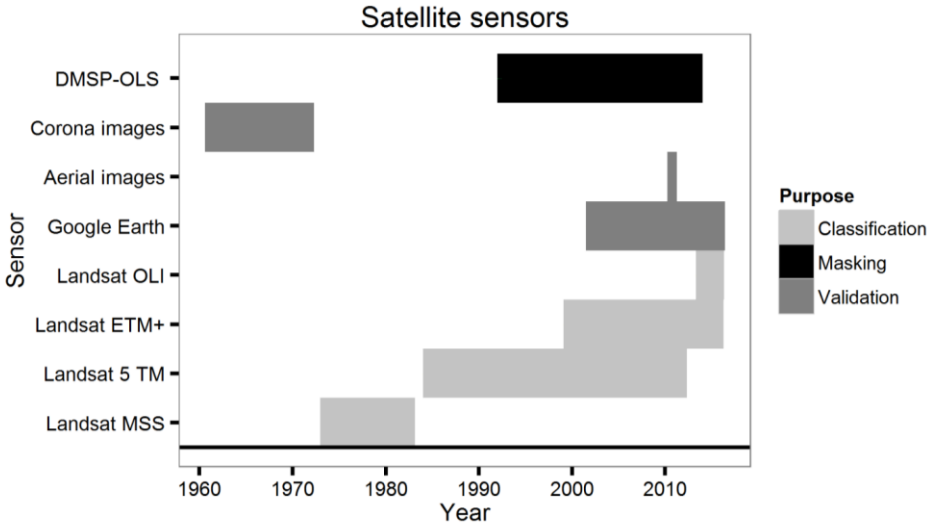

Figure 3. Timeline illustrating the satellite sensors used in this study, their purpose (classification, masking and validation) and date range.

Urban areas were masked out due to their apparent spectral similarity with urban and agricultural areas, using the DMSP OLS at 1 km resolution. This dataset consists of cloud-free composites made using all the available archived data (Figure 3). We applied a threshold to annual composites

from 2012 to 2013, 2002 to 2003 and 1992 to 1993 to mask the 2014, 2004, and 1994 maps, respectively. The 1992–1993 composite was also used to mask out urban areas from the 1984 and 1975 maps, as this dataset is only available from 1992 onwards. However, using this dataset as a pre-1992 mask may have resulted in an overestimation of the urban class extent. Burnt areas were successfully excluded from the analysis by taking the median pixel of the composite images, but extents were quantified using single dry season scenes. Fire is not considered a major land cover change transition, because regularly occurring fires are known to primarily affect the understory of woodland savannahs (as opposed to stand replacing fires) [29].

2.4. Land Cover Change Analysis

For each land cover class, analysis of the spatial extent, changes in area, i.e., gains, losses, persistence, and transitions from one land cover class to another, were calculated as proposed by [50] using the IDRISI land change modeller [42]. Cross tabulation matrices comparing two different categorical maps between successively mapped periods, allowed transitions among classes to be identified and potential underlying change processes assessed, and were computed as the off-diagonal values of the cross tabulation matrix [50]. The four administrative regions encompassing the study area have contrasting proportions of land-use categories (i.e., State Protected and Small-scale agriculture on communal land, etc.), population sizes and densities, as well as geographic extents. This is expected to impact on the amount of land converted to the other land-uses. We therefore: (i) map and discuss land cover class changes for each region, and compare these with the results of related satellite-based studies; and (ii) assess the most important land cover class transition in relation to the different land-use categories for each region, with a view to identifying which categories are important in determining change [51].

Percentage of land cover class changed in relation to the study area was calculated as (Equation (1)):

$$\% \, Area = \left(\frac{Area \, changed \, for \, a \, class}{Total \, area \, of \, land \, cover \, map} \right) \times 100 \quad (1)$$

2.5. Proximal Variables of Change

To determine which factors were influential in explaining the mapped land cover changes, we quantified the predominant land cover change in relation to the distance from possible drivers of change (proximal variables). They included proximity to: (i) towns; (ii) villages; (iii) roads; and (iv) rivers (including major, minor, perennial and ephemeral). These variables were chosen based on [51]; major towns included the regional centres of Rundu, Katima Mulilo, Divundu, Oshikango and Eenhana, while minor town constituted all remaining settlements. Euclidian distance from each feature was computed, and the output was then divided into 5 km buffers in order to accurately capture the expected small-scale land cover changes. The amount of the land converted is calculated a percentage of each distance buffer and buffer overlap was not accounted for [52].

2.6. Accuracy Assessment

To assess the pilot study map accuracy, 50 randomly stratified points per class were generated for the 2014 map. These were then validated visually using Landsat satellite scenes, high resolution Google Earth satellite imagery, aerial photos and ground knowledge. Similarly, for the 1975 period map, 50 randomly stratified points per class, including the urban class, were generated and validated using MSS Landsat and Corona imagery. For both datasets, overall accuracy was calculated [42]. Alternatively, for the composite image land cover maps spanning the periods 1984–2014, half of the training data were reserved for processing an accuracy assessment; the urban class was excluded as it was masked. Then, for each map, a confusion matrix representing overall validation expected accuracy (error) was processed using the reserved data. Finally, a qualitative assessment of each land cover map was undertaken using all available imagery.

In order to further assess the accuracy of the land cover maps generated in this study, an area adjusted accuracy assessment was additionally processed as per the method proposed by [53]. Here, validation data is employed for estimating the adjusted change area and confidence intervals, please refer to Olofsson et al. [53] for a complete review of the methods. Post-classification results are summarized by change matrices, which show the extent of different land cover transitions (i.e., from one land cover category to another). To map changes between two points in time, the number of variables in the to-from change matrix is the number of land cover classes squared. Therefore, in order to avoid having a matrix with 49 classes (seven land cover classes were used in this study), the land cover maps were modified to represent only binary Woodland and Non-Woodland classes (i.e., all other classes were merged into the Non-Woodland class), resulting in only four transitions in the matrix (i.e., two no change "transitions" and two changes from woodland to non-woodland, and non-woodland to woodland). In addition, the Woodland class is also the class of primary interest, and therefore only the changes from Woodland to Non-Woodland were assessed for area adjusted accuracy. The pairs of maps were then overlaid to create changes maps. An accuracy assessment of the change map was performed using a stratified random sample (independent of the sample selected for the accuracy assessment of the single date maps). We determined the reference land cover using Landsat scenes.

3. Results and Discussion

3.1. Classification Accuracy

Overall classification error for the pilot study map was 94.0% for 2014. In the pilot study, for the sake of feasibility, we only conducted an accuracy assessment for the present day period (2014), and assumed that the accuracy for the historical maps would be similar. In effect, an accuracy assessment for historical thematic maps is complicated by the fact that only the most recently classified maps can genuinely be compared against temporally coincident validation datasets. Similarly, as the scenes used to develop the maps and validation datasets are often temporally mismatched, we assume that there may be discrepancies in observed and mapped land covers which will affect the results of the accuracy assessment. Overall classification error for the 1975 map was of 78%, however, lower classification accuracies are likely here as not all scenes were from the same period (i.e., one scene was acquired for 1973 and two for 1979). Validation overall accuracy (errors) using reserved training data were of 99.7%, 99.8% and 99.5%, for the periods 1984–1994, 1994–2004 and 2004–2014, respectively (Table S2).

The equations proposed by Olofsson et al. [53] were used to calculate the error-adjusted land change area estimate at the 95% confidence interval (please refer to [53] for details), for the Woodland to the non-Woodland class (Table 2). Error matrices for each period are provided in the supplementary material. Here we find that although the land cover maps show high accuracies, the User's accuracy of the change category was of 30%, 54%, 28%, and 58% for the periods 1975–1984, 1984–1994, 1994–2004 and 2004–2014, respectively (Table S3), suggesting that the change maps were not highly accurate. Further, the extent of change estimated from the change maps falls within the 95% confidence interval of the error-adjusted estimated area, except in 2004–2014 change map. Here, the mapped area of deforestation is found to be of 4624 km^2, with an error-adjusted estimate of deforestation and $\pm$95% confidence interval of 1556 $km^2 \pm 76$ km^2 (Table 2). In addition, the change map had an overall accuracy of 72% (Table S3), however, the producer's accuracy (omission), which concerns the probability that validation dataset is correctly mapped, showed high accuracy (100%) for deforestation. This suggests that user's accuracy associated with the deforestation class was problematic. The stratified estimator of the extent of deforestation (1556 km^2) is less than half of the area of mapped deforestation. The reason for this disparity can be identified from the error matrix: it shows that all of the proportions of extents of deforestation are omitted from the map (the estimated area proportions omitted from the deforestation class were 0 and 0, column 3 (deforestation) (Table S3)). Hence, the

error-adjusted estimate of the extent of deforestation adds this omitted deforested extent to the mapped area of deforestation because: (i) it reduces the estimated area of deforestation; and (ii) had there been errors of omission, the estimated area of deforestation and 95% confidence interval would have been larger. Finally, for the 2004–2014 change map, the omission error associated with a few sample units of deforestation has a strong influence on the estimated area of deforestation i.e., every sample unit of omission error from the woodland class confers 1556 km^2 of deforestation. Similarly, each sample unit of omission error from the agricultural class confers roughly 211 km^2 of deforestation to the total error-adjusted value.

Table 2. The error-adjusted area of change (i.e., the transition from the Woodland to the Non-Woodland class), the 95% confidence interval of the error-adjusted estimated area, and actual change calculated from the change map.

Date	Change Estimate (km^2)	Error (km^2)	Actual Change (km^2)
1975–1984	577	20	5906
1984–1994	2161	159	7411
1994–2004	678	300	8653
2004–2014	1556	76	4624

3.2. Limitations

Numerous factors contribute to inaccuracies when classifying satellite imagery, especially in savannah environments [54–56]. To address these issues, we created composite images composed of all the available Landsat scenes for a single year to remove noise, included an NDVI band, and interactively classified these into the main cover types using knowledge gained from previous field visits and high resolution imagery. In addition, many limitations exist when applying hard classification techniques to heterogeneous vegetation biomes such as savannahs [57]. To this effect, object-based image classification of savannah vegetation has shown promising results [58,59]. The highest classification accuracies are associated with homogenous land covers, while heterogeneous land covers comprising vegetation with variable structures (i.e., grass, shrubs and trees of savannahs), have lower accuracies. Simply put, the primary reasons behind misclassifications are small land cover patch size (i.e., forest or grassland) and landscape heterogeneity [57,60]. Land cover maps divide the landscape into distinct classes, but in savannahs, land cover type boundaries are not necessarily distinct. Instead, they are often distinguished by a range of vegetation functional types, patches and spatial and temporal shifts from open grassland savannah to closed forest covers. These shifts result from numerous factors, including fire, variable rainfall, grazing and anthropogenic impacts such as deforestation and urbanization [25]. The inherent landscape variability coupled with, the pronounced woodland deciduousness, is therefore presumed to have contributed to the low accuracy assessment results for the change maps [25,61,62]. Furthermore, the agricultural landscape is composed of a mosaic of different land uses and land covers, leading to potential mis-classifications and confusions with other land cover classes, i.e., the "Wetland" and "Woodland" classes (Table S4). Finally, we assume that both the Woodland and Agriculture classes are highly heterogeneous and composed of numerous different plant functional groups (Table 1). Accordingly, the results presented must be interpreted with caution and as a best estimate of the aerial extents of these classes over time.

3.3. Change Area, Distribution and Transitions

Over the whole study period (1975–2014), the most extensive land cover class to change was woodland. Between 1975 and 2014, woodland area declined by −460,689 ha (4.3% of the study area), while agricultural land increased by 431,545 ha (4% of the study area) during that same period. The extents of all classes, as well as losses and gains in the Agriculture and Woodland classes are plotted for the entire study area (Figure 4).

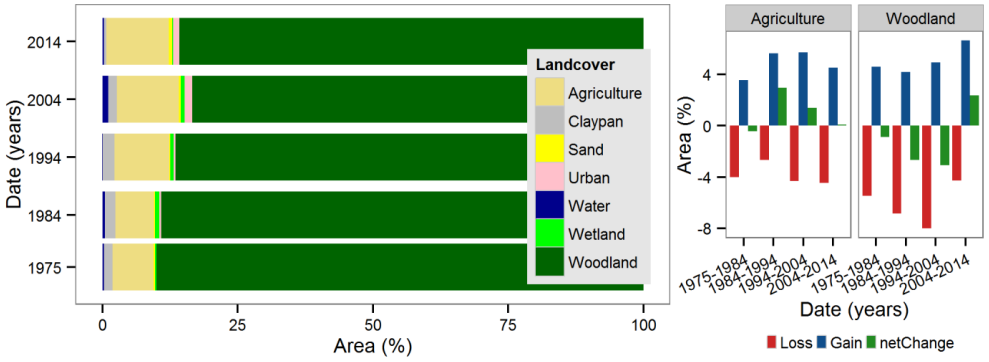

Figure 4. Bar graph illustrating the extents of the main land cover classes as a percentage of the study area (study area = 107,994 km^2) at decadal time scales. It shows an overall decline in the Woodland class and concurrent increase in the Agricultural class until 2004, followed by an increase in the Woodland class and decrease in the Agricultural class. Also included are the losses, gains and net change in the Agriculture and Woodland classes.

The overall trend for the whole study period was of a loss in woodland and an associated increase in agricultural classes except during the last decade, where woodland cover appears to be increasing. For all land cover classes, losses and gains took place simultaneously, i.e., between 1975 and 1984 woodland lost −5.47% and gained 4.59%, resulting in a net change of −0.87% of the study area. The pattern is similar for the intervals 1984–1994 and 1994–2004, however, between 2004 and 2014, woodland gains (6.64%) outweigh losses (−4.28%), resulting in a net positive change of 2.36%. Similarly, we see that during the 1994–2004 period, the highest woodland cover loss (−8%) was accompanied by the most important agricultural expansion (5.71%). For the whole study area, the predominant land cover transitions at each time interval were changes from woodland to agricultural classes, followed by changes from agricultural to woodland classes. For example, the predominant change trajectory between 1975 and 1984 as a percentage of the study area, included agriculture to woodland (3.54%) and woodland to agriculture (3.06%). These findings imply the woodland and agricultural land cover classes are dynamic and changeable, exhibiting relatively large losses, gains and exchanges over the intervals compared (Table S4). Correspondingly, 73% of the study area underwent no change; yet it is very likely that minor land cover changes, such as forest fires, could have taken place between study intervals. We mapped burnt area for each interval using the same approach but with single scenes from May to August, and found increases from 3.3% of the study area in 1975 to 11.5% in 1994, but constituted only 0.1% and 0.6% in 2004 and 2014, respectively.

The composite DSMP OLS images reveal urban area increased from 0.3% to 1.42% of the study area between 1994 and 2004, respectively. Urban areas experienced significant growth since the 1990s, in fact, Namibia's urban population more than doubled between 1981 and 2001 [39]. As shown by the change matrix (Table S4), increases in the extent of urban areas (1994–2004) resulted mainly in the loss of agricultural land, while urban expansion in the latter period (2004–2014) primarily caused woodland losses. However, changes in the spatial extent of urban areas should be interpreted with caution, as urban growth may not always be linked with electricity [29]. Nevertheless, this method provides an alternative method for estimating of the extent of human influence on the landscape.

Our analysis revealed a gradual reduction in the area of woodland and an increase in agricultural and urban land covers. Woodland conversion to agricultural land uses occurs as a continuous small-scale (2 ha) process of extraction and utilization of resources, driven by a need for permanent grazing pasture, construction timber and fire wood, and arable land for rain-fed cropping [17,29] (Figure 5a,b). Correspondingly, the process of cropland fallowing and subsequent woodland succession is constrained by diverse factors, chief among them being water availability, soil nutrient depletion, alterations and diminution of seedbanks, increased likelihood of fire disturbance and continual grazing pressure [38] (Figure 5c,d).

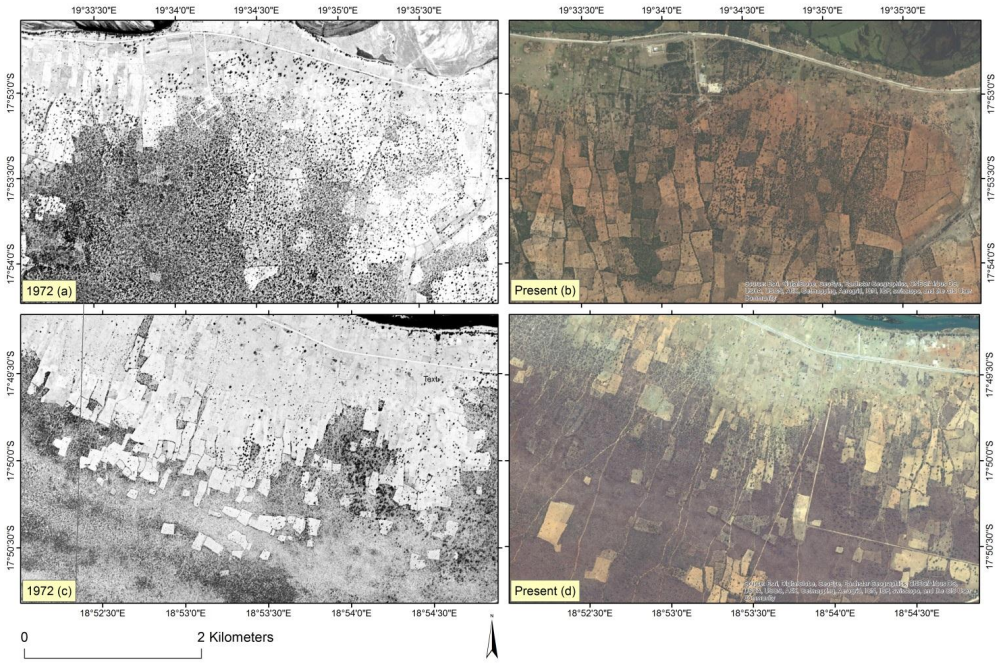

Figure 5. Corona image from 1972 (**a**) compared with present day satellite imagery (**b**) revealing small-scale agricultural growth (i.e., Woodland class loss); and a Corona image from 1972 (**c**) compared to present day satellite imagery (**d**) showing woodland succession and crop land fallowing (i.e., Woodland class gain).

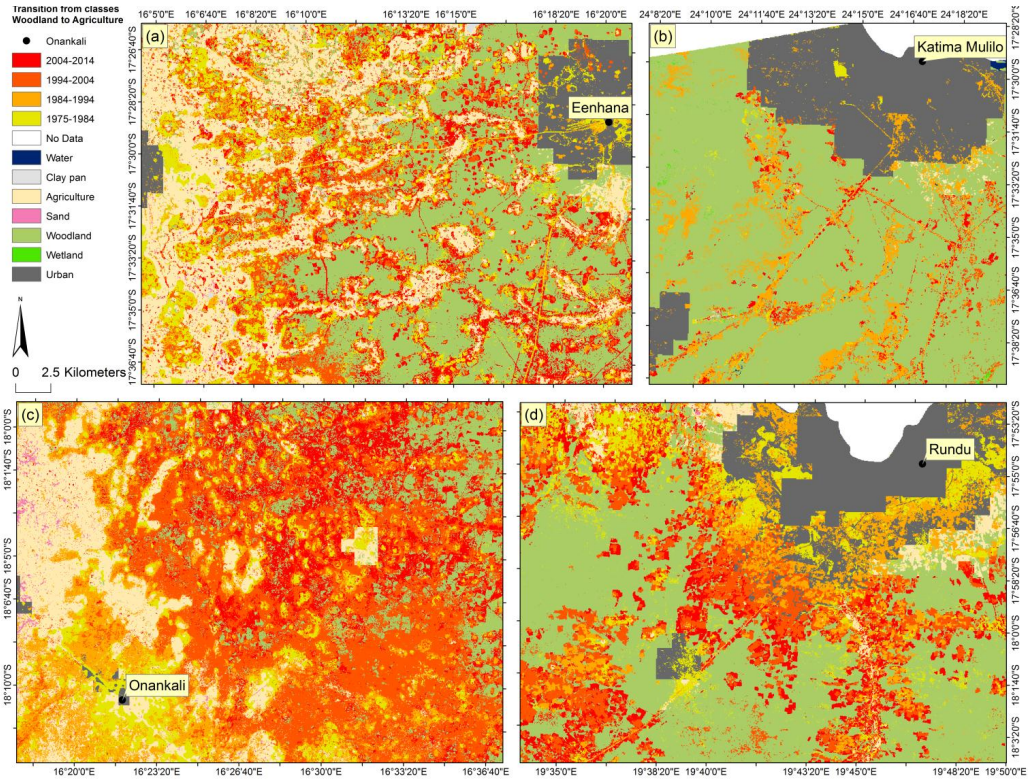

Figure 6. (**a**–**d**) Maps show the transitions from the classes Woodland to Agriculture for each time interval: yellow (19751984), orange (1984–1994), dark orange (1994–2004) and red (2004–2014). The encroachment the Agricultural class into the Woodland class as well as the nature of the changes, are evident for each time interval.

Figure 6 displays land cover maps for the main land cover class transition (i.e., Woodland to Agriculture classes) for each time interval: yellow (1975–1984), orange (1984–1994), dark orange (1994–2004) and red (2004–2014). The encroachment the Agricultural class into the Woodland class as well as the small-scale nature of the changes, are clearly visible for each time interval. For example, gradual decreases can be noted in proximity to the urban area of Rundu, which suggest urban expansion and small-scale cropping (Figure 6).

3.4. Land Cover Changes per Administrative Region

The administrative regions assessed vary importantly in terms of land-use categories, populations and geographic extents [39]. We therefore expect to find differences in the relative amounts of change. In effect, the Woodland class persistently declined in Ohangwena region, with consistent net losses. A similar pattern is evident for Oshikoto and Caprivi regions; however, a net positive change is evident for the 2004–2014 era (Figure 7).

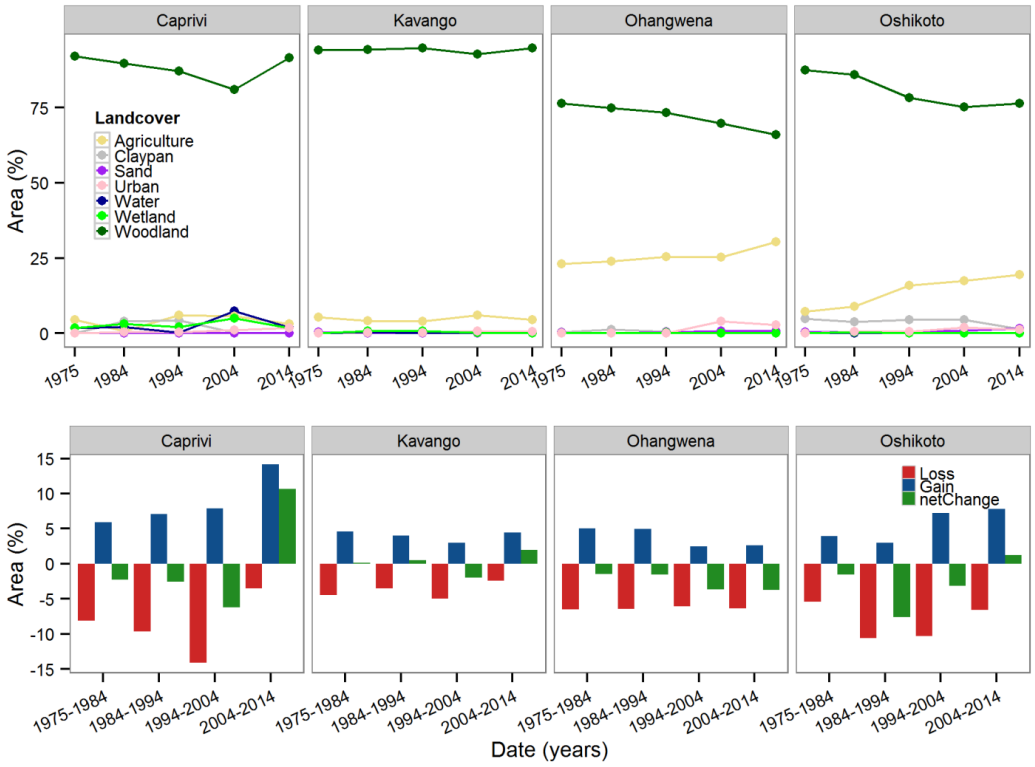

Figure 7. Plots showing the extent of all land cover classes (**above**) and the changes (i.e., losses, gains and net change) of the woodland cover class (**below**), by administrative region.

Contrastingly, Kavango region showed a gradual increase from 94.20%, 94.31%, 94.80%, 92.81% and 94.78% in 1975, 1984, 1994, 2004 and 2014, respectively (Figure 5). These results stand in contrast to studies finding decreases in woodland cover within the region of Kavango and therefore should be interpreted with caution [18,28–30]. Our results are likely due to a number of different factors, including: (i) the selection of broad land cover classes, i.e., Woodland and Agriculture, which encompass and range of different cover types, which are themselves highly susceptible to changes from anthropogenic and climatic drivers [63,64]; (ii) the method used to validate the maps, here, the earliest map (1975) was validated using a limited number of sample points, while the maps for the following eras were validated using half of the training data in combination with a qualitative assessment of each land cover map (Figure 2B); and (iii) the different temporal and spatial scales of the analyses. For example, the study by Erkkilä et al. [28] focused on a small portion of the Ohangwena

region and found decreases in woodland. The study by Röder et al. [29] centred upon the town and Rundu and encompassed part of the Eastern and Western Kavango provinces (Namibia) and part of the Cuando-Cubango province (Angola) covering an area of 15,000 km^2, at two time intervals (1990 and 2010). Had this study encompassed the entire region, their results may have been comparable. Further, Mendelsohn (2003) [18] find that for Kavango region, 26,140 ha of woodland were cleared by 1943, then, 72,100 ha (1.48%) in 1972 and 194,550 ha in 1996 (3.99%), resulting in a mean annual rate of increase of 3.9% from 1943 and 1996, but does not indicate which aerial imagery or satellite data were used. In comparison, for the same region, we found that in 1975, agricultural land constituted 260,839 ha (5.35%), and in 1994, it constituted 189,378 ha (3.89%), or a very similar mapped extent. The most important differences occur in 1970s period and may be attributable to the low spatial resolution (60 m) and variable quality of the MSS images used in this study [65]. Similarly, Pröpper et al. [30] found decreases in woodland cover for Kavango but do not provide exact aerial extents. We propose our results are likely due to both vegetation succession and woody encroachment occurring in areas previously dominated by grassland cover [66–68].

The predominant land cover class transition (i.e., Woodland to Agriculture) is assessed in relation to the different land-use categories, in order to identify which categories are the most important contributors to change for each region. Figure 8 shows the predominant transition as a percentage of each administrative region, for every land-use category. It is evident that for all regions, the greatest proportion occurs on "small scale agriculture on communal land", this is particularly obvious for Ohangwena region (Figure 8). Similarly, for all regions except Caprivi, we find that "large scale agriculture on communal land" is the third largest contributor to the predominant land cover transition. For Caprivi, Kavango and Oshikto, the second largest proportion of changes occurred on State Protected land (Ohangwena has no protected areas), suggesting land cover change impacts sites of conservation interest. Monitoring land cover changes in protected is essential, indeed, loss of habitat by deforestation and conversion to arable land are likely the most important threats to biodiversity [69]. As demonstrated by [70], detection of land cover changes, especially in mixed vegetation types such as grass and shrub land, is essential for facilitating numerous conservation activities, including the enforcement of protection and contributing to the work of managers and conservation scientists.

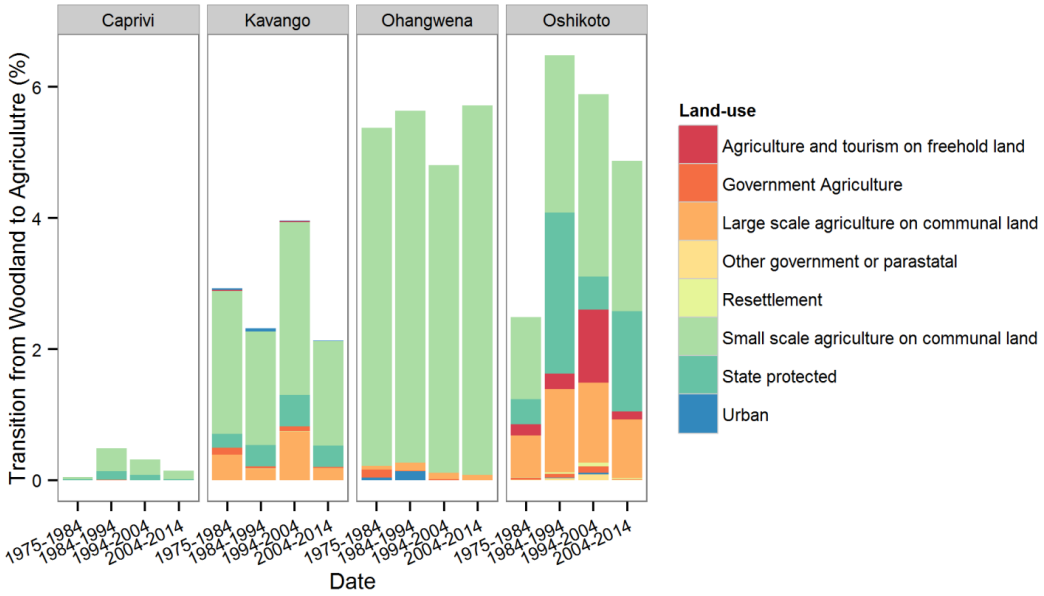

Figure 8. The predominant land cover transition (i.e., from Woodland to Agriculture) as a percentage of each administrative region, for every land-use category.

3.5. Drivers, Consequences and Implications of Land Cover Changes

The observed trends in woodland extent are likely explained by the current and historical Namibian socio-political context. Northern Namibia has benefited from a period of political and social stability and a strong drive for economic growth as of independence in 1990 [71]. This is evidenced by the expansion of the urban areas, for example, Rundu within the study area. The associated development of modern road networks has heightened the flow of goods between markets throughout the region, and consequently also access to and commercialization of communally held resources including, timber, pasture, thatch and access to remoter arable lands [29,39,72]. The majority of conversions from woodland to agricultural land cover classes, in terms of area, took place in the first two buffer zones in proximity to villages, rivers and roads, and the area of changes decreased with distance from these. For example, for the period 2004–2014, conversions from woodland to agricultural land in buffers zone 1 for "minor town", "major town" "rivers" and "roads" were of 4.56%, 1.95%, 4.88% and 4.03%, respectively. Except for "major towns", these values are more than double the values from the further zones, thus highlighting the correlation between proximity to villages, roads, and rivers and conversions from the woodland to the agricultural class. This analysis used the predominant land cover class transition (i.e., woodland to agriculture), and variables included proximity of villages, rivers and roads. The area of change decreased with increasing distance from all proximal variables, as evidence by significant Pearson's product-moment correlation coefficients (Table S5). All variables exhibit a clear and similar pattern (except distance to major towns), where the most important rates of conversion are found adjacent to the variable, and decrease with growing distance (Figure 9). As an avenue for future research, modelling transitions between categories as functions of environmental variables should be considered.

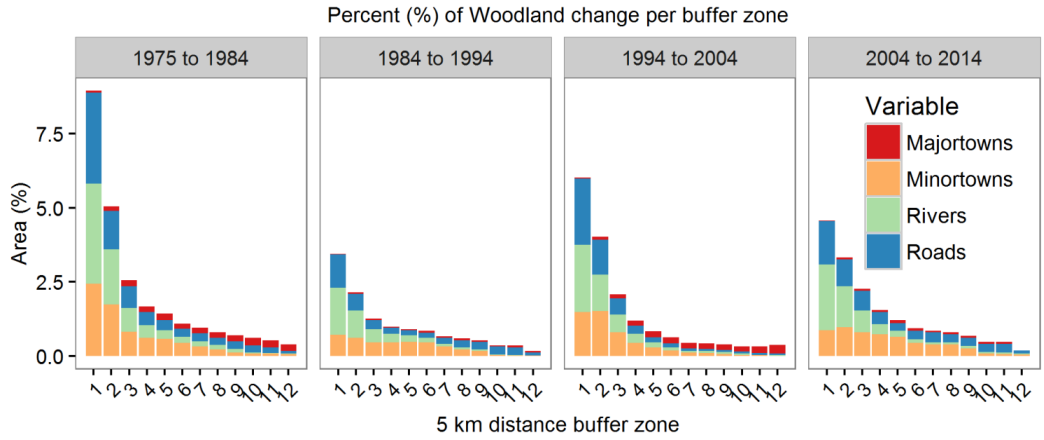

Figure 9. Bar graphs show the area of the predominant land cover class transition (i.e., woodland to agriculture per 5 km distance zone), as a percentage of each buffer zone, for each proximal change variable (i.e., rivers, roads, villages and major towns), calculated using Euclidean distance.

To illustrate this, ephemeral and perennial rivers are associated with more fertile, arable soils; in fact, river courses have been shown to be the preferred location for subsistence agriculture because of the higher soil fertility and access to water [73]. Ephemeral and major rivers, as well as floodplains, including the Okavango River and Cuvelai basin, respectively, have historically been regional centres of agriculture [73,74]. Importantly, therefore, the area available of potentially arable land is limited and decreasing.

The conversion of land to intensive, conventional agricultural uses on the continent is clearly exposed by recent, continental scale land cover studies [14,75]. In NE Namibia, however, woodland losses appear to be chiefly the result of small-scale subsistence farming (Figure 8). These changes are explained as being the result of expanding population pressure, better access to and commodification

of natural resources, as well as an ineffective legislation to manage land use and its distribution [29]. However, the observed trend of woodland conversion to subsistence agriculture is described as being unsustainable because, as subsistence agriculture spreads into increasingly marginal areas (in terms of agricultural potential and soil fertility), as a result of an ever decreasing amount of arable land, it increases the likelihood of soil becoming nutrient depleted sooner, thereby accentuating the need for more arable land [74]. An additional issue identified by various authors is the increased competition for grazing and other resources within commonage areas between wealthy farmers, who can afford both more stock and man power, and resident subsistence farmers [76]. Wealthy land users have been shown to be responsible for fencing off large tracts of commonage, often to the detriment of local residents. The enclosure of large tracts of woodland which were previously held as commonage, reduces the grazing intensity and woodland clearing within the enclosed area, however, these processes are in all likelihood displaced elsewhere [39]. In consequence, the increasing competition for land and grazing resources may be driving local land-use intensification, in the form of increased woodland clearing for cropping and resource extraction. In this context and given their wide extent, savannah woodland biomes are globally significant and constitute an important carbon sink if appropriately managed. Because of their potential for carbon sequestration, investments in the conservation and management of woodlands can provide African countries with benefits from carbon trading [77–79]. Although African savannahs provide for the livelihoods of a great many people, their capacity to furnish environmental services is not well understood and numerous constraints act to preclude their development, including a lack of valuation studies for such services, poorly defined tenure and markets, and a shortage of technical and institutional resourcefulness [80].

4. Conclusions

This study successfully develops a regional scale analysis of land cover change over four decades in NE Namibia. By processing and comparing multi-sensor Landsat scenes over five time intervals between 1975 and 2014, and across four administrative regions in NE Namibia, we observe an overall trend towards a reduction in woodland extent. The conversion of woodlands to arable land was the prevailing land cover transition process in terms of area, during all intervals, followed to a lesser extent by the succession of agricultural land to woodland. These transitions suggest that woodland clearing, followed by arable land abandonment and woodland succession, are widespread. The variable classification results obtained in the final analyses highlight the complexities of applying post classification change detection methods to spatially and temporally heterogeneous woodland savannah environments which are heavily impacted by grazing, fire and woodland clearing over decadal time scales [55,56]. The clearing and conversion of woodlands to other land uses appears to be primarily driven by subsistence-based, rain-fed cropping, with pastoralism, timber extraction, but also urban and infrastructural expansion, such as the creation of new roads, forming an integral part of the change process [29]. In effect, we look at the predominant land cover changes in relation to distance from towns, villages, rivers and roads, and find most changes occurred in proximity to these, and decrease with distance from these. Furthermore, the predominant land cover changes were found to occur mainly within land designated as communally held, followed by state protected land, suggesting land cover changes had a relatively high impact on conservation areas [70]. Finally, a lack of concise tenure rights regulating access to commonage grazing land may, in part, be driving the intensification of land-use. Here, subsistence farmers are compelled to compete for resources (primarily grazing and arable land) with wealthier farmers, who also often have the assets to fence large tracts of commonage, resulting in some areas, in what many perceive to be a typical "tragedy of the commons" situation. NE Namibia has extensive tracts of woodland savannah which provide numerous globally significant ecosystem services, such as carbon sequestration and biodiversity conservation, but also a wealth of natural resources critical to the livelihoods of communities in the region [38].

Ecosystems around the world are continuously changing as a result of anthropogenic and natural causes. In the present study, we investigate abrupt changes from one land cover class to another.

However, ecosystem changes can also be gradual, with subtle changes in vegetation and surface biophysical properties occurring even over short time scales [11]. The availability of new satellite archives at dense temporal resolutions present novel opportunities to study these changes, through the analysis of trends in land surface dynamics. In effect, time-series analyses which have typically been carried out on dense temporal and coarse spatial resolution sensors such as MODIS and AVHRR, are now applicable to high resolution datasets, for example, by combining Landsat 8 and Sentinel-2 archives [81]. Identifying and understanding the continual changes to our planet is essential for informing policy makers, managers and stakeholder about which ecosystems are at risk, what actions can be taken to better manage them and finally how effective these management actions might have been [82,83].

Supplementary Materials: The following are available online at http://www.mdpi.com/2072-4292/8/8/681/s1, Table S1: Google Earth Engine code, Table S2: Evaluation error matrixes indicating overall accuracy, errors of commission and omission, and total training data pixels, Table S3: Error matrices for each period showing adjusted change area and confidence intervals. The transition from woodland to non-woodland is labelled deforestation. Error matrix entries are expressed as the estimated area proportion. Map classes represent rows and reference classes the columns, Table S4: Cross tabulation matrices showing change trajectories as a percentage of the study area [50], Table S5: Pearson Pearson's coefficient (r) showing the relation between the aerial extent of main land cover class transition (i.e., woodland to agriculture) in each 5 km distance zone, and each proximal change variable for each interval assessed.

Acknowledgments: We would like to thank Katharine Wingate and Chris Barrat for their proof reading, Brice Prudat, Romie Nghitevelekwa, Laura Weidmann and Cornelis van der Waal for their assistance with fieldwork, Peter Scarth for his academic guidance, as well as the anonymous reviewers for their constructive review comments. We are also indebted to the numerous friends and acquaintances as well as colleagues from organisations that provided assistance in the field, logistical support and advice, including the Centre for African Studies (Basel), the Ministry of Agriculture, Water and Forestry, the Ministry of Environment and Tourism (Namibia) and the Desert Research Foundation of Namibia. The project was funded by a Humer Foundation Scholarship (Humer-Stiftung zur Förderung des wissenschaftlichen Nachwuchses), a Freiwillige Akademische Gesellschaft (University of Basel) grant and an Australian Endeavour Research Fellowship to Vladimir Wingate. No funds were received to cover the costs of publishing in open access.

Author Contributions: V. Wingate designed the study, produced the datasets, collected the field data, carried out the analyses, interpreted the results, created the figures and wrote the manuscript. All other authors supervised the designing of the study, discussed the results and edited the manuscript.

Conflicts of Interest: The authors declare no conflict of interest. The founding sponsors had no role in the design of the study; in the collection, analyses, or interpretation of data; in the writing of the manuscript, and in the decision to publish the results.

References

1. Foley, J.A.; Defries, R.; Asner, G.P.; Barford, C.; Bonan, G.; Carpenter, S.R.; Chapin, F.S.; Coe, M.T.; Daily, G.C.; Gibbs, H.K.; et al. Global consequences of land use. *Science* **2005**, *309*, 570–574. [CrossRef] [PubMed]
2. Tilman, D.; Fargione, J.; Wolff, B.; D'Antonio, C.; Dobson, A.; Howarth, R.; Schindler, D.; Schlesinger, W.H.; Simberloff, D.; Swackhamer, D. Forecasting agriculturally driven global environmental change. *Science* **2001**, *292*, 281–284. [CrossRef] [PubMed]
3. Matson, P.A. Agricultural intensification and ecosystem properties. *Science* **1997**, *277*, 504–509. [CrossRef] [PubMed]
4. Vitousek, P.M.; Mooney, H.A.; Lubchenco, J.; Melillo, J.M. Human domination of Earth's ecosystems. *Science* **1997**, *277*, 494–499. [CrossRef]
5. DeFries, R.; Achard, F.; Brown, S.; Herold, M.; Murdiyarso, D.; Schlamadinger, B.; de Souza, C. Earth observations for estimating greenhouse gas emissions from deforestation in developing countries. *Environ. Sci. Policy* **2007**, *10*, 385–394. [CrossRef]
6. Ellis, E.C.; Ramankutty, N. Putting people in the map: Anthropogenic biomes of the world. *Front. Ecol. Environ.* **2008**, *6*, 439–447. [CrossRef]
7. DeFries, R.S.; Foley, J.A.; Asner, G.P. Land-use choices: Balancing human needs and ecosystem function. *Front. Ecol. Environ.* **2004**, *2*, 249–257. [CrossRef]

8. Olofsson, P.; Kuemmerle, T.; Griffiths, P.; Knorn, J.; Baccini, A.; Gancz, V.; Blujdea, V.; Houghton, R.A.; Abrudan, I.V.; Woodcock, C.E. Carbon implications of forest restitution in post-socialist Romania. *Environ. Res. Lett.* **2011**, *6*, 045202. [CrossRef]
9. DeFries, R.S.; Houghton, R.A.; Hansen, M.C.; Field, C.B.; Skole, D.; Townshend, J. Carbon emissions from tropical deforestation and regrowth based on satellite observations for the 1980s and 1990s. *Proc. Natl. Acad. Sci. USA* **2002**, *99*, 14256–14261. [CrossRef] [PubMed]
10. Schulz, J.J.; Cayuela, L.; Echeverria, C.; Salas, J.; Rey Benayas, J.M. Monitoring land cover change of the dryland forest landscape of Central Chile (1975–2008). *Appl. Geogr.* **2010**, *30*, 436–447. [CrossRef]
11. Coppin, P.; Jonckheere, I.; Nackaerts, K.; Muys, B.; Lambin, E. Review article digital change detection methods in ecosystem monitoring: A review. *Int. J. Remote Sens.* **2004**, *25*, 1565–1596. [CrossRef]
12. Lu, D.; Mausel, P.; Brondízio, E.; Moran, E. Change detection techniques. *Int. J. Remote Sens.* **2004**, *25*, 2365–2401. [CrossRef]
13. Vittek, M.; Brink, A.; Donnay, F.; Simonetti, D.; Desclée, B. Land cover change monitoring using Landsat MSS/TM satellite image data over West Africa between 1975 and 1990. *Remote Sens.* **2014**, *6*, 658–676. [CrossRef]
14. Baccini, A.; Goetz, S.J.; Walker, W.S.; Laporte, N.T.; Sun, M.; Sulla-Menashe, D.; Hackler, J.; Beck, P.S.A.; Dubayah, R.; Friedl, M.A.; et al. Estimated carbon dioxide emissions from tropical deforestation improved by carbon-density maps. *Nat. Clim. Chang.* **2012**, *2*, 182–185. [CrossRef]
15. Bodart, C.; Brink, A.B.; Donnay, F.; Lupi, A.; Mayaux, P.; Achard, F. Continental estimates of forest cover and forest cover changes in the dry ecosystems of Africa between 1990 and 2000. *J. Biogeogr.* **2013**, *40*, 1036–1047. [CrossRef] [PubMed]
16. UN Food and Agriculture Organisation. *Global Forest Resource Assessment*; UN Food and Agriculture Organisation: Rome, Italy, 2010.
17. Erkkilä, A. Living on the land: Change in forest cover in north-central Namibia 1943–1996. *Int. J. Afr. Hist. Stud.* **2001**, *35*, 625–626.
18. Mendelsohn, J.M.; El Obeid, S. *Sand and Water: A Profile of the Kavango Region*; Struik: Cape Town, South Africa, 2003.
19. Miles, L.; Newton, A.C.; DeFries, R.S.; Ravilious, C.; May, I.; Blyth, S.; Kapos, V.; Gordon, J.E. A global overview of the conservation status of tropical dry forests. *J. Biogeogr.* **2006**, *33*, 491–505. [CrossRef]
20. Kasperson, R.E.; Archer, E.R. Vulnerable peoples and places. In *Ecosystems and Human Well-Being: Current State and Trends: Findings of the Condition and Trends Working Group*; Island Press: Washington, DC, USA, 2005; Volume 1, p. 143.
21. Verlinden, A.; Kruger, A.S. Changing grazing systems in central North Namibia. *Land Degrad. Dev.* **2007**, *18*, 179–197. [CrossRef]
22. Verlinden, A.; Seely, M.K.; Hillyer, A. Settlement, trees and termites in central North Namibia: A case of indigenous resource management. *J. Arid Environ.* **2006**, *66*, 307–335. [CrossRef]
23. Geiss, W. *A Preliminary Vegetation Map of Namibia*; Namibia Scientific Society: Windhoek, Namibia, 1971.
24. Scholes, R.; Archer, S. Tree-grass interactions in savannas. *Annu. Rev. Ecol. Syst.* **1997**, *28*, 517–544. [CrossRef]
25. Asner, G.P.; Lobell, D.B. A biogeophysical approach for automated SWIR unmixing of soils and vegetation. *Remote Sens. Environ.* **2000**, *74*, 99–112. [CrossRef]
26. Jung, M.; Henkel, K.; Herold, M.; Churkina, G. Exploiting synergies of global land cover products for carbon cycle modeling. *Remote Sens. Environ.* **2006**, *101*, 534–553. [CrossRef]
27. Herold, M.; Mayaux, P.; Woodcock, C.; Baccini, A.; Schmullius, C. Some challenges in global land cover mapping: An assessment of agreement and accuracy in existing 1 km datasets. *Remote Sens. Environ.* **2008**, *112*, 2538–2556. [CrossRef]
28. Erkkilä, A.; Löfman, S. Forest cover change in the Ohangwena region, northern Namibia: A case study based on multitemporal Landsat images and aerial photography. *South. Afr. For. J.* **1999**, *184*, 25–32. [CrossRef]
29. Röder, A.; Pröpper, M.; Stellmes, M.; Schneibel, A.; Hill, J. Assessing urban growth and rural land use transformations in a cross-border situation in northern Namibia and southern Angola. *Land Use Policy* **2015**, *42*, 340–354. [CrossRef]

30. Pröpper, M.; Gröngröft, A.; Falk, T.; Eschenbach, A.; Fox, T.; Gessner, U.; Hecht, J.; Hinz, M.O.; Huettich, C. Causes and perspectives of land-cover change through expanding cultivation in Kavango. In *Biodiversity in Southern Africa. Volume 3: Implications for Landuse and Management*; Klaus Hess Publishers: Göttingen, Germany; Windhoek, Namibia, 2010.
31. Hüttich, C.; Gessner, U.; Herold, M.; Strohbach, B.J.; Schmidt, M.; Keil, M.; Dech, S. On the suitability of MODIS time series metrics to map vegetation types in dry savanna ecosystems: A case study in the Kalahari of NE Namibia. *Remote Sens.* **2009**, *1*, 620–643. [CrossRef]
32. Strohbach, B.J.; Petersen, A. Vegetation of the central Kavango woodlands in Namibia: An example from the mile 46 livestock development centre. *S. Afr. J. Bot.* **2007**, *73*, 391–401. [CrossRef]
33. Verlinden, A.; Laamanen, R. Modelling woody vegetation resources using Landsat TM imagery in northern Namibia. *S. Afr. For. J.* **2006**, *207*, 27–39.
34. Campbell, B.; Angelsen, A.; Cunningham, A.; Katerere, Y.; Sitoe, A.; Wunder, S. *Miombo Woodlands—Opportunities and Barriers to Sustainable Forest Management*; CIFOR: Bogor, Indonesia, 2007; Available online: http://www.cifor.cgiar.org/miombo/docs/Campbell_BarriersandOpportunities.pdf (accessed on 4 November 2008).
35. Wang, L.; D'Odorico, P.; Ringrose, S.; Coetzee, S.; Macko, S.A. Biogeochemistry of Kalahari Sands. *J. Arid Environ.* **2007**, *71*, 259–279. [CrossRef]
36. National Planning Commission. *Namibia 2011 Population and Housing Census Preliminary Results*; National Planning Commission: Windhoek, Namibia, 2012.
37. Verlinden, A.; Dayot, B. A comparison between indigenous environmental knowledge and a conventional vegetation analysis in North Central Namibia. *J. Arid Environ.* **2005**, *62*, 143–175. [CrossRef]
38. Mendelsohn, J.M.; El Obeid, S. *Forests and Woodlands of Namibia*; RAISON: Windhoek, Namibia, 2005.
39. Mendelsohn, J.M.; El Obeid, S. *The Communal Lands in Eastern Namibia*; RAISON: Windhoek, Namibia, 2002.
40. Verlinden, A.; Laamanen, R. Long term fire scar monitoring with remote sensing in northern Namibia: Relations between fire frequency, rainfall, land cover, fire management and trees. *Environ. Monit. Assess.* **2006**, *112*, 231–253. [CrossRef] [PubMed]
41. United States Geological Survey. Available online: https://www.usgs.gov/ (accessed on 1 June 2014).
42. Eastman, J. *IDRISI Selva*; Clark University: Worcester, MA, USA, 2012.
43. Google Earth Engine. Available online: https://developers.google.com/earth-engine/ (accessed on 1 June 2014).
44. Singh, A. Review article digital change detection techniques using remotely-sensed data. *Int. J. Remote Sens.* **1989**, *10*, 989–1003. [CrossRef]
45. Colwell, J.E.; Weber, F. Forest change detection. In Proceedings of International Symposium on Remote Sensing of Environment, Ann Arbor, MI, USA, 11–15 May 1981; pp. 839–852.
46. Gislason, P.O.; Benediktsson, J.A.; Sveinsson, J.R. Random forests for land cover classification. *Pattern Recognit. Lett.* **2006**, *27*, 294–300. [CrossRef]
47. Breiman, L.; Friedman, J.; Stone, C.J.; Olshen, R.A. *Classification and Regression Trees*; CRC Press: Boca Raton, FL, USA, 1984.
48. Breiman, L. Random forests. *Mach. Learn.* **2001**, *45*, 5–32. [CrossRef]
49. Elvidge, C.D.; Cinzano, P.; Pettit, D.R.; Arvesen, J.; Sutton, P.; Small, C.; Nemani, R.; Longcore, T.; Rich, C.; Safran, J.; et al. The Nightsat mission concept. *Int. J. Remote Sens.* **2007**, *28*, 2645–2670. [CrossRef]
50. Pontius, R.G.; Shusas, E.; McEachern, M. Detecting important categorical land changes while accounting for persistence. *Agric. Ecosyst. Environ.* **2004**, *101*, 251–268. [CrossRef]
51. Mendelsohn, J. *Atlas of Namibia: A Portrait of the Land and Its People*; New Africa Books (Pty) Ltd.: Cape Town, South Africa, 2002.
52. Geist, H.J.; Lambin, E.F. Proximate causes and underlying driving forces of tropical deforestation. *BioScience* **2002**, *52*, 143–150. [CrossRef]
53. Olofsson, P.; Foody, G.M.; Stehman, S.V.; Woodcock, C.E. Making better use of accuracy data in land change studies: Estimating accuracy and area and quantifying uncertainty using stratified estimation. *Remote Sens. Environ.* **2013**, *129*, 122–131. [CrossRef]
54. Shao, G.; Wu, J. On the accuracy of landscape pattern analysis using remote sensing data. *Landsc. Ecol.* **2008**, *23*, 505–511. [CrossRef]

55. Hill, M.J.; Hanan, N.P.; Hoffmann, W.; Scholes, R.; Prince, S.; Ferwerda, J.; Lucas, R.M.; Baker, I.; Arneth, A.; Higgins, S. Remote sensing and modeling of savannas: The state of the dis-union. In Proceedings of the 34th International Symposium on Remote Sensing of the Environment (ISRSE), Sydney, NSW, Australia, 10–15 April 2011.
56. Hanan, N.P.; Hill, M.J. Challenges and opportunities for improved remote sensing and modelling of global savannas. In Proceedings of Earth Observation for Land-Atmosphere Interaction Science, Frascati, Italy, 3–5 November 2010.
57. Smith, J.H.; Stehman, S.V.; Wickham, J.D.; Yang, L. Effects of landscape characteristics on land-cover class accuracy. *Remote Sens. Environ.* **2003**, *84*, 342–349. [CrossRef]
58. Whiteside, T.G.; Boggs, G.S.; Maier, S.W. Comparing object-based and pixel-based classifications for mapping savannas. *Int. J. Appl. Earth Obs. Geoinform.* **2011**, *13*, 884–893. [CrossRef]
59. Johansen, K.; Arroyo, L.A.; Armston, J.; Phinn, S.; Witte, C. Mapping riparian condition indicators in a sub-tropical savanna environment from discrete return lidar data using object-based image analysis. *Ecol. Indic.* **2010**, *10*, 796–807. [CrossRef]
60. Smith, J.H.; Wickham, J.D.; Stehman, S.V.; Yang, L. Impacts of patch size and land-cover heterogeneity on thematic image classification accuracy. *Photogramm. Eng. Remote Sens.* **2002**, *68*, 65–70.
61. Gessner, U.; Machwitz, M.; Conrad, C.; Dech, S. Estimating the fractional cover of growth forms and bare surface in savannas. A multi-resolution approach based on regression tree ensembles. *Remote Sens. Environ.* **2013**, *129*, 90–102. [CrossRef]
62. Childes, S.L. Phenology of nine common woody species in semi-arid, deciduous Kalahari sand vegetation. *Vegetatio* **1988**, *79*, 151–163. [CrossRef]
63. Vicente-Serrano, S.; Cabello, D.; Tomás-Burguera, M.; Martín-Hernández, N.; Beguería, S.; Azorin-Molina, C.; Kenawy, A. Drought variability and land degradation in semiarid regions: Assessment using remote sensing data and drought indices (1982–2011). *Remote Sens.* **2015**, *7*, 4391–4423. [CrossRef]
64. Asner, G.P.; Elmore, A.J.; Olander, L.P.; Martin, R.E.; Harris, A.T. Grazing systems, ecosystem responses, and global change. *Annu. Rev. Environ. Resour.* **2004**, *29*, 261–299. [CrossRef]
65. Chander, G.; Markham, B.L.; Helder, D.L. Summary of current radiometric calibration coefficients for Landsat MSS, TM, ETM+, and EO-1 ALI sensors. *Remote Sens. Environ.* **2009**, *113*, 893–903. [CrossRef]
66. Ward, D. Do we understand the causes of bush encroachment in African savannas? *Afr. J. Range Forage Sci.* **2005**, *22*, 101–105. [CrossRef]
67. O'Connor, T.G.; Puttick, J.R.; Hoffman, M.T. Bush encroachment in southern Africa: Changes and causes. *Afr. J. Range Forage Sci.* **2014**, *31*, 67–88. [CrossRef]
68. Mitchard, E.T.A.; Flintrop, C.M. Woody encroachment and forest degradation in sub-Saharan Africa's woodlands and savannas 1982–2006. *Philos. Trans. R. Soc. Lond. B Biol. Sci.* **2013**, *368*, 20120406. [CrossRef] [PubMed]
69. Pimm, S.L.; Jenkins, C.N.; Abell, R.; Brooks, T.M.; Gittleman, J.L.; Joppa, L.N.; Raven, P.H.; Roberts, C.M.; Sexton, J.O. The biodiversity of species and their rates of extinction, distribution, and protection. *Science* **2014**, *344*, 1246752. [CrossRef] [PubMed]
70. Szantoi, Z.; Brink, A.; Buchanan, G.; Bastin, L.; Lupi, A.; Simonetti, D.; Mayaux, P.; Peedell, S.; Davy, J. A simple remote sensing based information system for monitoring sites of conservation importance. *Remote Sens. Ecol. Conserv.* **2016**, *2*, 16–24. [CrossRef]
71. Malan, J. *Guide to the Communal Land Reform Act, 2002*; Land, Environment, and Development Project, Legal Assistance Centre, and the Advocacy Unit, Namibia National Farmers' Union: Windhoek, Namibia, 2009.
72. Mendelsohn, J. *Farming Systems in Namibia*; Research & Information Services of Namibia: Windhoek, Namibia, 2006.
73. Gröngröft, A.; Luther-Mosebach, J.; Landschreiber, L.; Eschenbach, A. Mashare soils. *Biodivers. Ecol.* **2013**, *5*, 105–108. [CrossRef]
74. Oldeland, J.; Erb, C.; Finck, M.; Jürgens, N. *Environmental Assessments in the Okavango Region*; BEE, Biocentre Klein Flottbek and Botanical Garden, University of Hamburg: Hamburg, Germany, 2013.
75. Hansen, M.C.; Potapov, P.V.; Moore, R.; Hancher, M.; Turubanova, S.A.; Tyukavina, A.; Thau, D.; Stehman, S.V.; Goetz, S.J.; Loveland, T.R.; et al. High-resolution global maps of 21st-century forest cover change. *Science* **2013**, *342*, 850–853. [CrossRef] [PubMed]

76. Mendelsohn, J. *Customary and Legislative Aspects of Land Registration and Management on Communal Land in Namibia*; Ministry of Land and Resettlement and European Union: Windhoek, Namibia, 2008.
77. Zahabu, E.; Skutsch, M.M.; Sosovele, H.; Malimbwi, R.E. Reduced emissions from deforestation and degradation. *Afr. J. Ecol.* **2007**, *45*, 451–453. [CrossRef]
78. Jindal, R.; Swallow, B.; Kerr, J. Forestry-based carbon sequestration projects in Africa: Potential benefits and challenges. *Nat. Resour. Forum* **2008**, *32*, 116–130. [CrossRef]
79. Bond, I.; Chambwera, M.; Jones, B.; Chundama, M.; Nhantumbo, I. *REDD+ in Dryland Forests Issues and Prospects for Pro-Poor REDD in the Miombo Woodlands of Southern Africa*; International Institute for Environment and Development (UK): London, UK, 2010.
80. Chidumayo, E.N.; Gumbo, D.J. *The Dry Forests and Woodlands of Africa: Managing for Products and Services*; Earthscan: London, UK, 2010.
81. Drusch, M.; Del Bello, U.; Carlier, S.; Colin, O.; Fernandez, V.; Gascon, F.; Hoersch, B.; Isola, C.; Laberinti, P.; Martimort, P. Sentinel-2: ESA's optical high-resolution mission for GMES operational services. *Remote Sens. Environ.* **2012**, *120*, 25–36. [CrossRef]
82. Kuenzer, C.; Dech, S.; Wagner, W. Remote sensing time series revealing land surface dynamics: Status quo and the pathway ahead. In *Remote Sensing Time Series*; Springer: Basel, Switzerland, 2015; pp. 1–24.
83. Pettorelli, N.; Vik, J.O.; Mysterud, A.; Gaillard, J.M.; Tucker, C.J.; Stenseth, N.C. Using the satellite-derived NDVI to assess ecological responses to environmental change. *Trends Ecol. Evol.* **2005**, *20*, 503–510. [CrossRef] [PubMed]